P1.13 USING MULTI-SPECTRAL SATELLITE REMOTE SENSING TECHNIQUES TO NOWCAST NOCTURNAL CONVECTION INITIATION

Wayne M. MacKenzie, Jr.* and John R. Mecikalski
University of Alabama in Huntsville, Huntsville, Alabama

INTRODUCTION

Accurately forecasting convection initiation (CI) is an ongoing problem within meteorology today. Mecikalski and Bedka (2005) have demonstrated with good success a process which nowcasts (0-1 hour) convection initiation during the daytime using GOES real-time satellite processing. Using 1 km visible imagery, temporal temperature trends using multiple wavelengths and band differencing, an algorithm was developed to select regions where cumulus clouds have ~60% or greater chance of precipitating within the next hour. An ongoing extension of this work is to advance daytime CI nowcasting to nighttime conditions. Since 1 km visible satellite is not available during the nighttime hours, one must rely on infrared channels with a spatial resolution of 4 km to monitor clouds. This can be challenging because 4 km is less than the cumulus horizontal spatial scale initially and tracking cumulus at night is more difficult. As a corollary, during nighttime conditions the 3.9 micron near-infrared channel becomes available as an additional resource to use.

BACKGROUND

Mecikalski and Bedka (2005) developed a research and operational system for use during daytime hours which utilizes GOES Imager satellite data to track and monitor the evolution of cumulus clouds. Using a cumulus cloud mask they are able to classify clouds into five categories: fair weather cumulus, towering cumulus, cumulus with small anvils, thin cirrus and thick cirrus. Then using the areas where fair weather cumulus and towering cumulus are identified, and using a satellite wind tracking algorithm developed by Velden et. al (1997, 1998), and modified by Bedka and Mecikalski (2005) for obtaining "mesoscale" flows, the cumulus clouds are monitored temporally. Then using information developed from Roberts and Rutledge (2003) to monitor the cumulus cloud growth within a multi-spectral satellite framework.

Roberts and Rudledge (2003) as well as Mecikalski and Bedka (2005) have developed a list of infrared multi-spectral band differencing techniques as interest fields within a pre-CI cumulus cloud. A detailed discussion of the physical characteristics of the multi-spectral band differencing are not discussed here and can be found within the Roberts and Rudledge (2003) and Mecikalski and Bedka (2005) studies. However, Table 1 contains the useful band differencing techniques, their contribution and critical values used during the day which will be adapted to be used at night within this study in addition to the use of the 3.9 micron channel. Convection initiation is defined as the first time a convective cell reaches a reflectivity of 35 dBZ on the radar (Mecikalski and Bedka, 2005). This definition will be used within this study.

GOES-12 Derived Field	Contribution	Critical Values
10.7 μm Brightness Temp. (T_B)	Cloud-top temperature assessment	<0°C
6.7-10.7 μm Difference	Cloud-top height relative to tropopause	-35°C to -10°C
13.3-10.7 μm Difference	Cloud-top height changes	-25°C to -5°C
10.7 μm temporal trend	Cloud-top cooling rates	<-4°C/15 mins ΔT_B/30 mins< ΔT_B/15 mins
6.7-10.7 μm temporal change	Time changes in cloud height relative to the tropopause	>3°C/15 mins
13.3-10.7 temporal change	Time changes in cloud top height	>3°C/15 mins

Table 1. Adapted from Mecikalski and Bedka (2005). This table Includes a list of CI interest

---

**Corresponding Author's Address:*
Wayne M. MacKenzie, Jr., Department of Atmospheric Science, University of Alabama in Huntsville, National Space Science & Technology Center, 320 Sparkman Drive, Huntsville, AL 35802; e-mail: wayne.mackenzie@nsstc.uah.edu.

fields which are going to be carried over from the daytime studies to nighttime study. The contributions to each field as well as the critical values are listed for the GOES-12 satellite system.

The 3.9 micron near-infrared channel within the GOES Imager, as well as the 10.7 micron channel, are frequently used for the identification of fog and stratus clouds during the night (Ellrod et al., 1989; Ellrod, 1991; Nelson and Ellrod, 1996; Ellrod, 1995; Lee, 2000; Dostalek et al., 1997). Without the visible channels, it is often difficult to identify low-level clouds. The 3.9 micron channel can assist with identification of low-level, water clouds because within this channel, emissivity values of water clouds are lower than the 10.7 micron channel. Water clouds contain small microphysical particle sizes which allows different brightness temperatures to be detected (Hunt, 1973). This is due to the 10.7 microns sensing all clouds close to blackbody temperature (due to emissivity values of clouds in the 10.7 micron channel greater than 0.9) and senses a warmer cloud top temperature whereas 3.9 micron channel senses much less than a blackbody for water clouds (Hunt, 1973) thus making the sensed temperature cooler. Differencing the 3.9 micron channel with the 10.7 micron channel will allow the determination of liquid water clouds and high cirrus clouds. A slight positive difference (~2-6K) is described as water clouds (e.g. fog, stratus, or low-level cumulus). A negative difference (greater than -8K) is described as ice clouds. Typically areas with no clouds have a difference around 0K, however a +/-1K error can occur due to the sensitivity of the 3.9 micron channel to surface emissivity as well as the sub-pixel sensitivity to heat (e.g. urban heat island effect) (RAMM, 1996). When clouds reach a temperature of approximately 250K, the error associated with the 3.9 micron channel reaches 2K, which is a limitation of the channel (RAMM, 1996). This is why the 3.9 micron channel appears to contain a lot of noise in thunderstorm cirrus due to the temperature uncertainty at cold temperatures.

METHODOLOGY

Processing non-stationary clouds over a 15 minute temporal resolution using 4 km spatial resolution is challenging. Our methodology consists of the following: First, the coldest pixel is the pixel which is tracked. The underlying assumption for this is that the coldest pixel is the updraft region of the storm. Then using three successive images which are selected starting with the earliest image where there is a discernable updraft (e.g. cold pixel). We wish to determine the wind speed and direction as early as possible before the convection reaches the influence of upper-level steering currents. Using the three successive images, we track the cells subjectively using McIDAS. This process of subject storm tracking is performed a total of five times using different parts of the coldest 4 km pixel. Then an average wind speed and direction are calculated. From that average wind speed and direction, u- and v-components of the wind are computed.

Using the assumptions that the wind direction and speed calculated does not change over time, and that the calculated wind speed and direction are the winds of the low-level cloud fields, we can determine an offset vector. This offset vector is used to back-track the cell in time to determine the evolution of the cloud field before precipitation and even before the cell developed into a mature cumulus.

Second, centering each image using the coldest pixel or the locations determined by the offset vector, brightness temperatures are retrieved within a 21 pixel by 21 pixel box and knowing each pixel is 1 km, the area of the box is 441 km^2 (The McIDAS grid is a 1 km grid even though the satellite data is 4 km resolution). It is the brightness temperatures within each 21 pixel by 21 pixel box which are used for analysis.

Errors associated with tracking the clouds will be minimal since the analysis performed is on a 1 km pixel whereas the data has a 4 km spatial resolution. Even though there may be an error with the location of a cloud on a 1 km grid (due to the use of 4 km data on the 1 km grid), the cloud still remains within a 4 km pixel observed by the satellite. Thus, the errors associated with tracking the clouds will not provide much of an error.

RESULTS

Using the process above, satellite band differencing and temporal band differencing were performed to determine whether the 3.9 micron channel can value-add the current CI nowcasting system. Preliminary results show that 3.9 micron channel is excellent at determining cloud top microphysics. The property of the 3.9 micron channel is that water clouds have a lower emissivity than ice clouds. This means that water clouds appear slightly cooler than the 10.7 micron channel. This usually means that band differencing the 3.9 micron channel with other channels will result in a larger difference.

The next section takes a look into one specific case and how well forecast this event could have been using the CI interest fields from Mecikalski and Bedka (2005) and with the addition of the 3.9 micron channel.

02 JUNE 2005

A case which occurred on 02 June 2005 where convective cells formed ahead of an approaching squall line in northeast Oklahoma will be examined. The convection reached 35 dBZ at 0243 UTC (Figure 1). Many of the Mecikalski and Bedka (2005) CI interest fields did reach their critical values (Table 1) approximately 1 hour and 15 minutes before CI time (Figures 2-7). The 10.7 micron channel first went below 0°C at 0130 UTC and remained below that temperature for the reminder of the time (Figure 2). The 10.7 micron channel temperature temporal trend well exceeded the critical value of <-4°C within a 15 minute period between 0115 UTC and 0130 UTC (Figure 3). The 6.5-10.7 micron channel difference was within the critical value at 0130 UTC (Figure 4). The temporal trend of the 6.5-10.7 micron channel difference attained the critical values at 0130 UTC (Figure 5). The 13.3-10.7 micron channel difference was well within the critical values at 0130 UTC (Figure 6) and the temporal trend of the 13.3-10.7 micron temperature difference was within the critical values between 0115 UTC and 0130 UTC (Figure 7). Precipitation first occurred on the radar at 0228 UTC however was below the criteria of 35 dBZ used to define CI and spatially was on the order of 1 km. The goal of this presentation is to examine what was the 3.9 micron channel response.

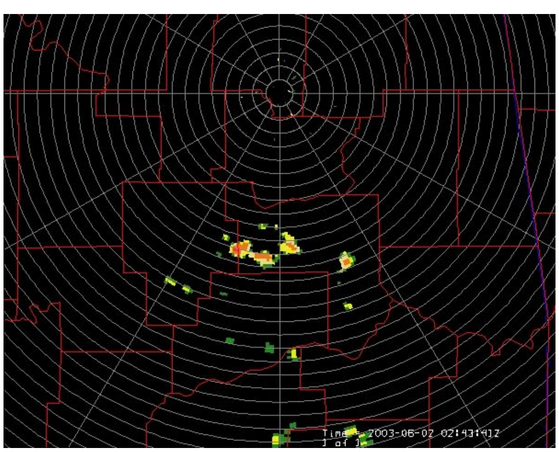

Figure 1. This radar image taken on 02 June 2005 at 0243 UTC from the Tulsa (KINX) radar site. Reflectivity values greater than 30 dBZ are plotted (yellow color is 35 dBZ) along with range rings from the radar site. The range rings are spaced every 5 km to show the spatial extend of the convection.

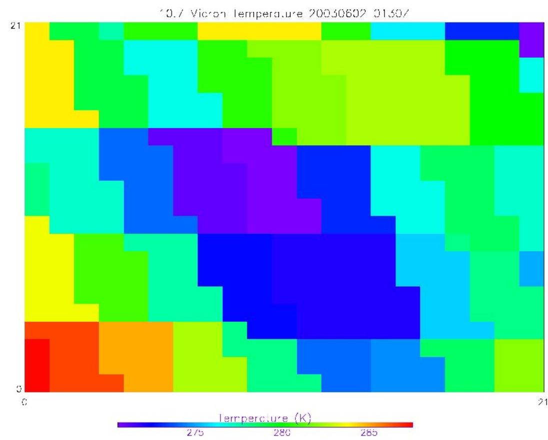

Figure 2. This is the 10.7 micron channel temperature from 02 June 2003 at 0130 UTC. The purple color corresponds to a temperature below 0°C.

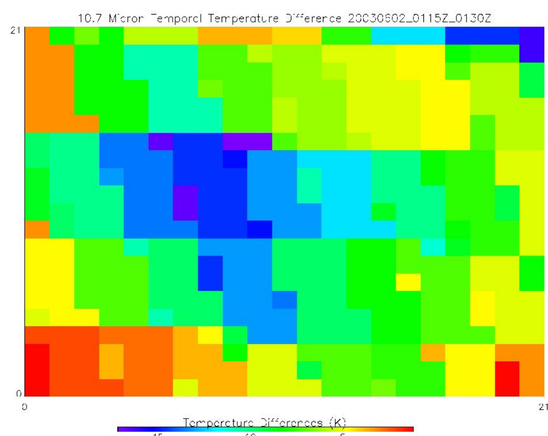

Figure 3. 10.7 micron channel time trend between 0115 UTC and 0130 UTC. The blue colors corresponds to a temperature difference of <-10°C per 15 minutes which exceeds the critical value of <-4°C.

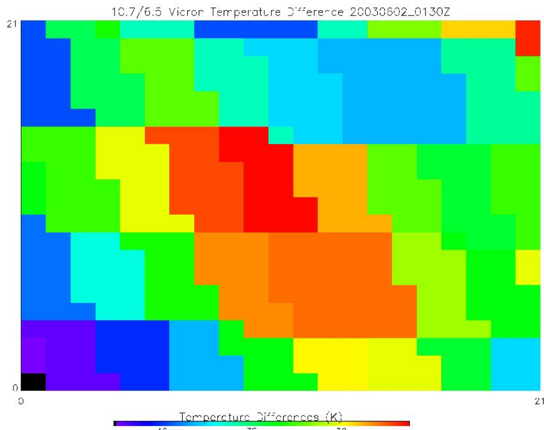

Figure 4. The 10.7-6.5 micron channel difference was within the critical values at 0130 UTC. The red colors correspond to a temperature difference of approximately -25ºC which is within the critical value for this interest field.

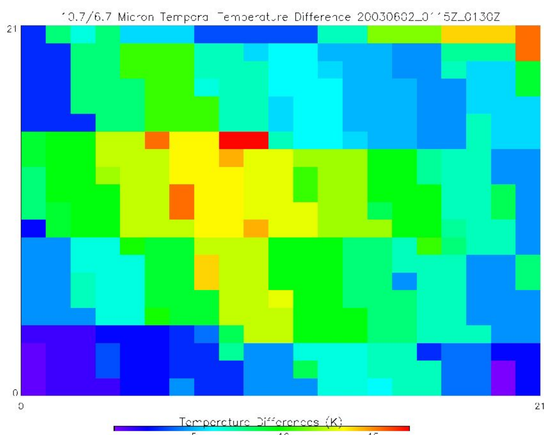

Figure 5. The 10.7-6.5 Micron Temporal Temperature Difference between 0115 UTC and 0130 UTC exceeded the critical values of > 3ºC within 15 minutes. The green colors corresponds to a temperature difference of 10ºC and the red colors corresponds to a temperature difference of 15ºC.

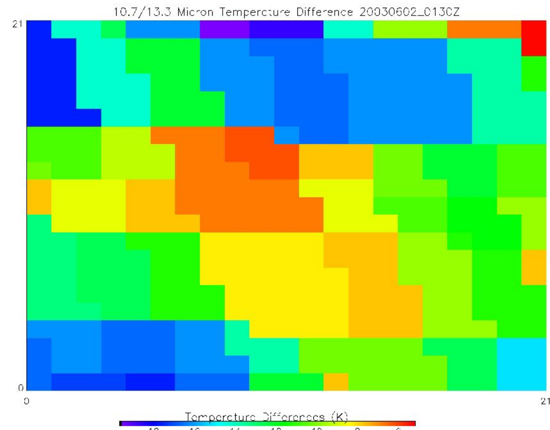

Figure 6. 10.7-13.3 micron channel difference at 0130 UTC. The temperature differences are well within the critical values of -25ºC to -5ºC. Every pixel within this image falls within the critical values.

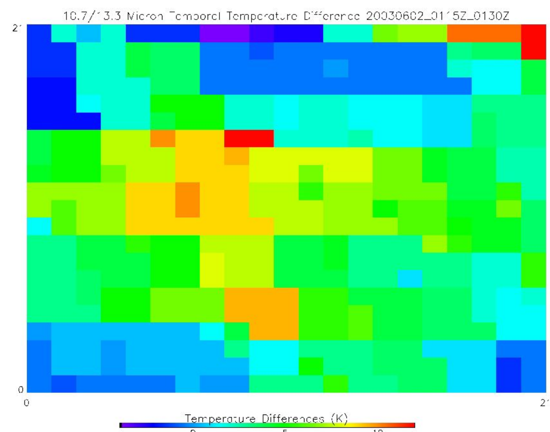

Figure 7. The temporal trend of the 10.7-13.3 micron channel difference between 0115 UTC and 0130 UTC. Values exceed the critical value of >3ºC within 15 minutes. Colors of green, yellow and red are pixels which meet the critical values.

The response from the 3.9 micron channel temporal trend followed that of 10.7 except for some minor difference which could be attributed to sensor diffraction (RAMM, 1996) and emissivity differences. The 3.9 micron channel was warmer than the 10.7 channel before CI as shown from a 10.7-3.9 micron channel difference (Figure 8). Since there was a positive difference, that tell us that the cloud top is water. When the temporal trend of the 10.7-3.9 micron channel difference fell to approximately -10ºC (Figure 9), the cloud has transformed from a liquid water cloud to an ice cloud at the top. Remember, the radar reflectivity of 35 dBZ occurred at 0243 UTC. Comparing Figure 9 to the radar image (Figure 1) you can see the outline of the storms. The darker blue and purple colors in Figure 9 correspond to updraft regions and colder cloud tops. The lighter blue corresponds to the thin cirrus from the convection. By 0315 UTC, the convection formed into a linear convective system similar to the image in Figure 9.

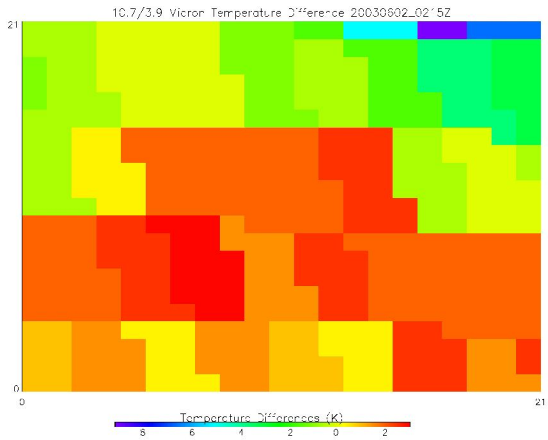

Figure 8. This 10.7-3.9 micron channel difference taken before CI, shows that the 3.9 micron is slightly warmer meaning that these clouds are water clouds. The red colors are areas of a positive difference.

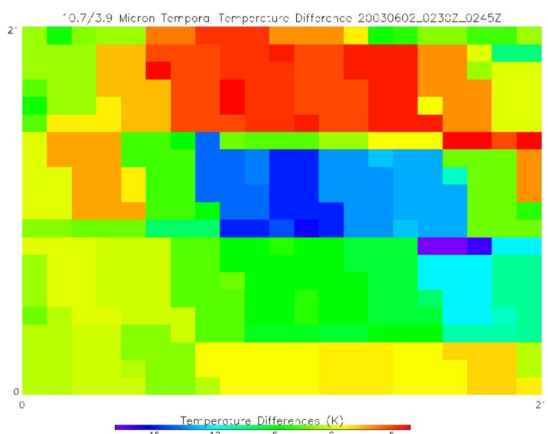

Figure 9. The temporal trend of the 10.7-3.9 micron channel difference taken at times 0230 UTC and 0245 UTC shows the negative differences which means the cloud has transformed from a liquid water cloud to ice at the cloud tops. The blue colors correspond to a strong negative difference. The blue color outlines the convection.

While more work needs to be done, it appears as if the 3.9 micron channel may be able to provide useful information. More cases are needed to determine if the 3.9 micron channel can be used as an interest field to nowcast CI. This case presented would have been nowcast one hour before any precipitation occurred and one hour and 15 minutes using the Mecikalski and Bedka CI definition.

FUTURE WORK

This work is in its infancy. Although five cases have been examined, only one case is presented here. The plan to further this research includes developing a statistically significant dataset of nocturnal CI cases to determine a possible criteria for nowcasting CI using the 3.9 micron channel. Several more cases will develop a set of statistics which can aid in determining critical values. Another use will be using MM5 model simulations to determine storm evolution with a few of these cases. This will provide insight into how the storms evolve and how the satellite responds to the evolution. Performing this analysis on many cases will give insight into how the 3.9 micron channel could provide information into the CI nowcasting system. Other uses of the 3.9 micron channel could include forecasting lightning development or precipitation development since the 10.7-3.9 micron channel difference provides information into cloud top microphysics.

ACKNOWLEGDMENTS

This project's goals coincide with those of the FAA Aviation Weather Research Program (AWRP) efforts at the National Center for Atmospheric Research (NCAR), to nowcast CI for the purpose of enhancing aviation safety. Thus, this presentation highlights recent research progress on a collaboration between the University of Alabama in Huntsville, the University of Wisconsin-Madison, Cooperative Institute for Meteorological Satellite Studies (UW-CIMSS) and NCAR to routinely diagnose convection over land and ocean regions. As proven techniques are developed through this collaboration, they will be transferred into the forecast systems supported by the FAA for nowcasting convection over land and oceans.

REFERENCES

Bedka, K.M. and J.R. Mecikalski, 2005: Application of satellite-derived atmospheric motion vectors for estimating mesoscale flows. Accepted in the *Journal of Applied Meteorology*.

Dostalek, J.F., J. Weaver, J. Purdom and K. Winston, 1997: Nighttime detection of low-level thunderstorm outflow using a GOES multispectral image product.

Wea.Forecasting,**12**, 947-950.

Ellord, G.P., 1991: Nighttime fog detection with bi-spectral GOES-VAS Imagery.P*roc., Fourth Int. Conf. on Aviation Weather Systems*, Paris, France. Amer. Meteor. Soc., 71-75.

_____, E. Maturi, and J. Steger, 1989: Detection of fog at night using dual channel GOES-VAS imagery. *Proc. 12th Conf. on Weather Analysis and Forecasting*, Monterey, CA, Amer. Meteor. Soc., 108-114.

_____, 1995: Advances in the detection and analysis of fog at night using GOES multispectral infrared imagery. *Wea. Forecasting*, **10**, 606-619.

Hunt, G.E., 1973: Radiative properties of terrestrial clouds at visible and infrared thermal window wavelengths. *Quart. J. Roy. Meteor. Soc.*, **99**, 346-369.

Lee, T.F., 2000: Nighttime observation of sheared tropical cyclones using GOES 3.9-µm data. *Wea. Forecasting*, **15**, 759-766.

Mecikalski, J.R., and K. Bedka, 2005: Forecasting convective initiation by monitoring the evolution of moving cumulus in daytime GOES imagery. Accepted to the "IHOP_2002 Convective Initiation Special Issue" of the *Monthly Weather Review*.

Nelson J.P., and G. Ellrod, 1996: Improved GOES-8 multispectral (10.7µm-3.9µm) satellite imagery to detect stratus and fog at night. *Proc. Eighth Conf. on Satellite Meteor. and Oceanography*, Atlanta, GA, Amer. Meteor. Soc., 172-176.

RAMM, 1996: GOES 3.9 µm channel tutorial. [Available online at http://www.cira.colostate.edu/ramm/goes39/cover.htm]

Roberts, R.D., and S. Rutledge, 2003: Nowcasting storm initiation and growth using GOES-8 and WSR-88D data. *Wea. Forecasting*, **18**, 562-584.

Veldon, C.S., C. Hayden, S. Nieman, W.Menzel, S. Wanzong, and J. Goerss, 1997: Upper-tropospheric winds derived from geostationary satellite water vapor observations. *Bull. Amer. Soc.,* **78**, 173-195.

Veldon, C.S., T. Olander, and S. Wanzong, 1998: The impact of multispectral GOES-8 wind information on Atlantic tropical cyclone track forecasts in 1995. Part I: Dataset methodology, description, and case analysis. *Mon. Wea. Rev.,* **126**, 1202-1218.